Research Article

Stacked Intelligent Metasurfaces: Wavefront Engineering for Extended Effective Radiative Near-Field Range in 6G Systems

Yajun Zhao[1,2]

1. ZTE Corporation, Shenzhen, China; 2. State Key Laboratory of Mobile Network and Mobile Multimedia Technology, China

Mid- to high-frequency near-field communications and sensing in 6G systems face fundamental limitations when implemented with conventional single-layer programmable metasurfaces. Under fixed physical aperture constraints, these structures suffer from insufficient degrees of freedom for wavefront manipulation, finite phase quantization accuracy, and inadequate capability to synthesize weak-curvature spherical wavefronts at extended distances. Consequently, their engineering-usable near-field range typically falls significantly short of the classical Rayleigh distance. This paper investigates stacked intelligent metasurfaces (SIMs) as a solution to extend the effective radiative near-field range while maintaining identical aperture size, feed configuration, and power constraints. First, we clarify that the Rayleigh distance represents an intrinsic physical boundary determined by aperture size and wavelength, fundamentally constrained by diffraction limits. The proposed "effective range enhancement" does not alter this boundary but reduces the gap between engineering performance and theoretical limits. Second, we establish an equivalent model of SIMs as programmable cascaded lens groups through unified geometrical and physical optics analysis, demonstrating how multilayer structures progressively reshape wavefront curvature via end-to-end joint optimization. Third, we develop a unified near-field model incorporating insertion loss, phase quantization error, and interlayer spacing deviations within a cascaded spherical-wave propagation framework. Numerical simulations validate that multilayer SIMs substantially improve focusing quality and extend the engineering-usable operating range throughout the Rayleigh region, providing theoretical foundation and design guidance for 6G near-field wireless systems.

Corresponding author: Yajun Zhao, zhao.yajun1@zte.com.cn

 doi.org/10.32388/VP6D01

I. Introduction

THE evolution toward mid- to high-frequency bands, extremely large-scale arrays, and integrated sensing and communication (ISAC) in 6G systems challenges conventional far-field plane-wave assumptions [1][2]. As array apertures grow significantly larger than operating wavelengths, an increasing number of users and targets fall within the radiative near-field region, where electromagnetic fields exhibit pronounced spherical wave characteristics with strong distance-dependent behavior [3]. Near-field technology enables joint distance-angle beam focusing, enhanced sensing precision, and novel spatial multiplexing mechanisms, establishing itself as a cornerstone for 6G advancement.

Despite the theoretical near-field region defined by Rayleigh distance theory, practical implementations using single-layer phased arrays or intelligent metasurfaces face severe limitations. Under fixed aperture constraints, their effective operating range typically constitutes only a fraction of the Rayleigh distance due to single-shot amplitude-phase coding constraints. This performance gap motivates the pursuit of architectures capable of maximizing near-field range utilization.

Reconfigurable intelligent surfaces (RISs) offer promising characteristics including low cost, power efficiency, and programmable electromagnetic response [4]. However, conventional RIS implementations function as single programmable thin lenses with limited wave manipulation capability, insufficient for complex near-field beamforming requirements [5]. Stacked intelligent metasurfaces (SIMs) address this limitation by cascading multiple programmable transmissive layers along the propagation direction, enabling electromagnetic waves to undergo sequential "modulation-propagation-remodulation" processes [6][7]. This architecture substantially enriches realizable wavefronts and enhances spatial field reconfiguration capabilities, supporting advanced functionalities such as spatial filtering and multi-beam generation [8].

While existing research has explored SIM advantages in wideband transceiver design [9] and capacity enhancement [10], a systematic understanding of their capability to extend effective radiative near-field range under fixed aperture constraints remains lacking. Crucially, the distinction between engineering performance boundaries and fundamental physical limits requires clarification.

The Rayleigh distance $R_{Ray} = 2D^2/\lambda$ serves as the conventional near-field/far-field boundary, where D represents aperture dimension and λ denotes wavelength. Fundamentally, this boundary arises from the nonuniform optical path difference of spherical waves across finite apertures. When the maximum phase difference induced by geometric path variations reaches $\pi/8$, plane-wave approximations become invalid [11]. This criterion establishes the Rayleigh distance not as an empirical definition but as the physical manifestation

of aperture diffraction limits, defining both the existence threshold for near-field effects and the boundary for range-domain resolution capability.

This paper systematically investigates transmissive SIMs' capability to extend effective radiative near-field range under fixed aperture constraints. Our contributions are threefold:

1. We establish an equivalent model of SIMs as programmable cascaded lens groups through unified geometrical and physical optics analysis, revealing the core mechanism: multilayer joint optimization forms an equivalent telescopic system that increases effective focal length and shifts the virtual source point backward, enabling spherical wavefront synthesis at extended distances.
2. We develop a unified near-field model for single-layer and multilayer transmissive metasurfaces within a cascaded spherical-wave propagation framework, explicitly incorporating insertion loss, phase quantization error, and interlayer spacing deviations.
3. We quantify SIM performance in extending engineering-effective radiative near-field operating range through rigorous numerical analysis, demonstrating significant improvements in focusing quality throughout the Rayleigh region.

The remainder of this paper is organized as follows: Section II defines system models and problem formulation; Section III elucidates the physical mechanism of near-field extension; Section IV presents theoretical modeling and mathematical derivation; Section V provides numerical validation; and Section VI concludes the work.

II. System Model and Problem Definition

A. System Architecture

Consider a transmitting system comprising K feeds and L transmissive metasurface layers, all sharing identical physical dimensions and element arrangements while stacked sequentially along the z-axis. For fair comparison, single-layer metasurfaces and multilayer SIMs are analyzed under identical operating frequency, total aperture size, feed configuration, and input power constraints. The model explicitly incorporates nonideal factors including cascaded insertion loss and phase quantization error to enable practical performance evaluation.

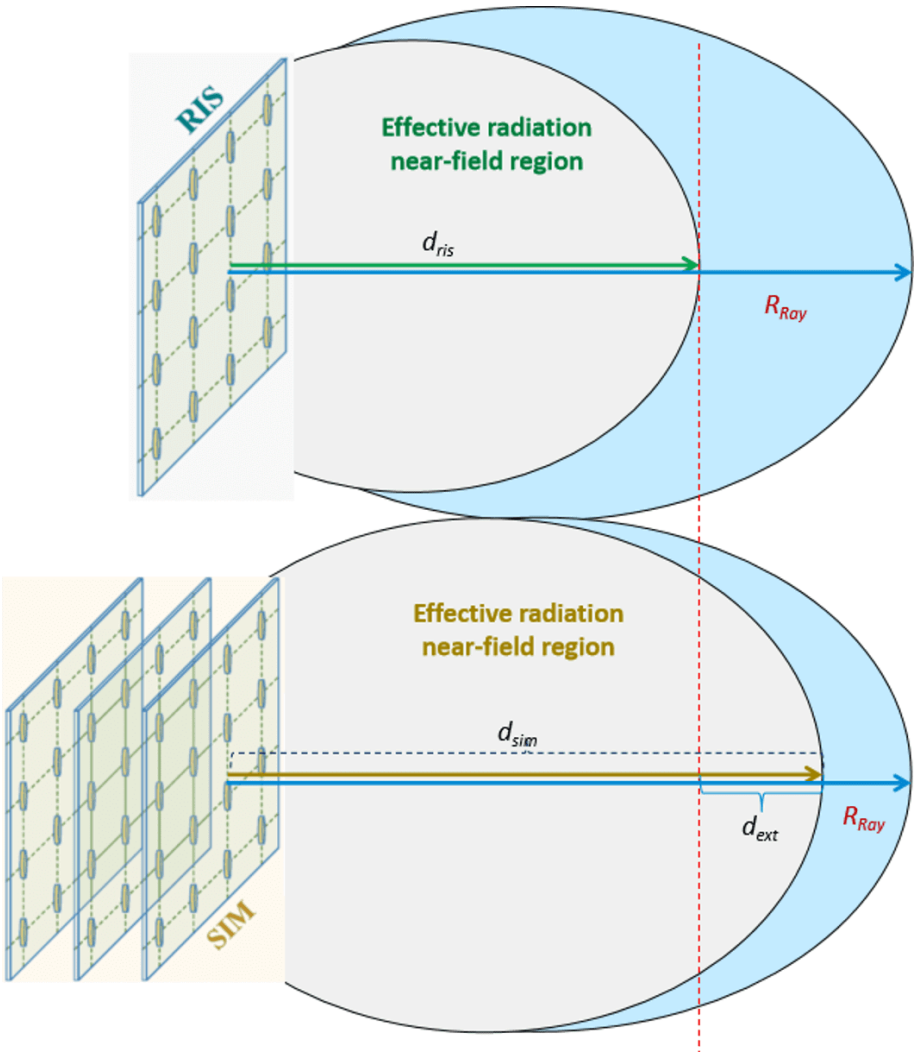

Figure 1. Schematic illustration of the radiative near field for a single-layer metasurface and a transmissive stacked intelligent metasurface.

Let the operating wavelength be λ, physical aperture size D, and each metasurface layer contain N programmable elements. With the aperture-center normal defining the z-axis, the observation point P is located at $(0, 0, r)$. The transverse coordinate of the nth element on the lth layer is $\rho_{l,n} = (x_{l,n}, y_{l,n})$, with complex transmission coefficient $t_{l,n} = \beta_{l,n} e^{j\varphi_{l,n}}$, where $\beta_{l,n}$ and $\varphi_{l,n}$ represent amplitude transmission coefficient and phase response, respectively.

B. Cascaded Spherical-Wave Propagation Model

The feed excitation vector s propagates through the system via cascaded transformations. The propagation matrix from feeds to the first layer is $G_{1,0} \in \mathbb{C}^{N \times K}$, while the lth layer's modulation matrix is the diagonal

doi.org/10.32388/VP6D01

matrix $\Phi_l = diag\left(\beta_{l,1}e^{j\varphi_{l,1}}, \ldots, \beta_{l,N}e^{j\varphi_{l,N}}\right)$. Free-space spherical-wave propagation between adjacent layers is modeled by matrices $G_{l+1,l} \in \mathbb{C}^{N\times N}$, and propagation to observation point P is represented by $G_{out}^{(L)}(r)$.

The equivalent transfer relation for an L-layer SIM at observation point P is:

$$H^{(L)}(r) = G_{out}^{(L)}(r)\Phi_L G_{L,L-1}\cdots\Phi_1 G_{1,0}. \tag{1}$$

The output field vector becomes:

$$y^{(L)}(r) = H^{(L)}(r)s. \tag{2}$$

Spherical-wave propagation between elements follows:

$$[G_{l+1,l}]_{n,m} = \frac{1}{d_{l+1,l}^{(n,m)}}\exp\left(-j\frac{2\pi}{\lambda}d_{l+1,l}^{(n,m)}\right), \tag{3}$$

where $d_{l+1,l}^{(n,m)}$ denotes Euclidean distance between elements.

This scalar-field model neglects polarization effects and strong mutual coupling, focusing on wavefront curvature control mechanisms central to our analysis.

C. Physical Definition and Intrinsic Boundary of Classical Radiative Near Field

The classical radiative near field originates from nonuniform optical path differences across finite apertures. For observation point $P = (0, 0, r)$, the maximum optical path difference between aperture edge and center is:

$$\Delta L_{\max}(r) = \sqrt{r^2 + \left(\frac{D}{2}\right)^2} - r. \tag{4}$$

Under paraxial condition $r \gg D$, this simplifies to:

$$\Delta L_{\max}(r) \approx \frac{D^2}{8r}. \tag{5}$$

The corresponding maximum phase difference becomes:

$$\Delta\varphi_{\max}(r) = \frac{2\pi}{\lambda}\Delta L_{\max}(r) \approx \frac{\pi D^2}{4\lambda r} \tag{6}$$

When this phase difference satisfies $\Delta L_{\max}(r) \approx \frac{D^2}{8r}$, the observation point exhibits pronounced near-field characteristics, yielding the Rayleigh distance:

$$R_{Ray} = \frac{2D^2}{\lambda}. \tag{7}$$

The Rayleigh distance embodies two inseparable physical meanings: (1) it defines the critical distance where intrinsic geometric phase difference reaches $\pi/8$, establishing the physical baseline for near-field effects; (2) it represents the absolute boundary imposed by aperture diffraction limits beyond which electromagnetic waves lose range-domain resolution capability.

D. Definition of Effective Radiative Near-Field Range

The classical Rayleigh distance characterizes physical boundaries but does not equate to engineering usability limits. We define the **effective radiative near-field range (ERF)** as the maximum distance where systems maintain sufficient near-field gain relative to reference configurations under prescribed performance-loss thresholds.

For observation point $P = (0, 0, r)$, let $E_{ideal}(r)$ represent the ideal near-field focusing reference field and $E^{(L)}(r)$ denote the normalized field generated by an L-layer structure. The normalized focusing coherence coefficient is:

$$\mu^{(L)}(r) = \frac{|\langle E^{(L)}(r), E_{ideal}(r) \rangle|}{\|E^{(L)}(r)\| \|E_{ideal}(r)\|}. \tag{8}$$

The focusing-gain loss becomes:

$$\varepsilon^{(L)}(r) = 1 - \mu^{(L)}(r). \tag{9}$$

Given admissible threshold $\varepsilon_{th} \in (0, 1)$, the effective radiative near-field range is:

$$R_{ERF}^{(L)} = \max \left\{ r \in [0, R_{Ray}] : \varepsilon^{(L)}(r) \leq \varepsilon_{th} \right\}. \tag{10}$$

This definition complements rather than conflicts with the classical Rayleigh distance, identifying engineering-useful distances within the physical near-field region.

III. Physical Mechanism of SIM Near-Field Extension

A. Single-Layer Metasurface Limitations

A single-layer transmissive metasurface functions analogously to a thin lens in geometrical optics. To achieve ideal focusing at distance F, the required phase distribution follows:

$$\varphi(\rho) = -\frac{2\pi}{\lambda} \left(\sqrt{F^2 + \rho^2} - F \right), \tag{11}$$

where F represents equivalent focal length and ρ denotes radial coordinate.

Three fundamental limitations constrain single-layer performance:

1. **Quantization precision constraints**: As focusing distance increases, required phase curvature flattens, making accurate synthesis of weak-curvature wavefronts challenging under finite-bit phase control.
2. **Single-shot transformation limitation**: Single-plane modulation cannot simultaneously achieve incident-field correction, curvature reshaping, and long-distance focusing, imposing theoretical bounds on wavefront synthesis accuracy.

3. **Lack of intermediate remodulation**: Post-modulation wavefront evolution follows propagation physics without opportunity for correction.

The maximum phase difference for single-layer structures decays monotonically with distance:

$$\Delta\varphi_{\max}^{SL}(r) \approx \frac{\pi D^2}{4\lambda r} \tag{12}$$

limiting engineering-effective range despite physical near-field existence.

B. Multilayer SIM: Programmable Cascaded Lens System

SIM architecture functions as a programmable cascaded lens group, where each metasurface layer serves as a programmable phase-modulation plane and interlayer propagation enables spherical-wave diffraction. Through "modulation-propagation-remodulation" cascading, wavefronts undergo progressive reshaping and precise regulation.

For a two-layer SIM with interlayer spacing s and equivalent focal lengths f_1, f_2, the combined focal length satisfies:

$$\frac{1}{f_{eq}} = \frac{1}{f_1} + \frac{1}{f_2} - \frac{s}{f_1 f_2}. \tag{13}$$

Crucially, performance gains arise not from mere layer stacking but from end-to-end joint optimization of multilayer phase configurations with interlayer propagation physics. This enables telescopic wavefront transformation: preceding layers perform wavefront preconditioning and incident-field correction, redistributing intermediate wavefront curvature and reducing phase-control burden for subsequent layers. Final layers then execute fine phase compensation, accurately synthesizing weak-curvature spherical wavefronts with reduced per-layer phase-gradient requirements.

The total phase difference between representative paths $\mathcal{P}_a$ and $\mathcal{P}_b$ at observation point P becomes:

$$\Delta\varphi_{SIM}(r) = \frac{2\pi}{\lambda}\Delta L_{geo}^{SIM}(r) + \Delta\varphi_{code}^{SIM} \tag{14}$$

where $\Delta L_{geo}^{SIM}(r)$ represents accumulated geometric path difference and Δ_{code}^{SIM} denotes equivalent coded phase difference. Expanding this expression:

$$\Delta\varphi_{SIM}(r) = \sum_{l=0}^{L}\frac{2\pi}{\lambda}\Delta L_l(r) + \sum_{l=1}^{L}\Delta\varphi_l \tag{15}$$

reveals that SIM maximum phase difference combines multisegment geometric differences with multilayer coded phase contributions, substantially exceeding single-layer capabilities.

C. Near-Field Extension Mechanism

The enhancement mechanism operates through three fundamental aspects:

1. **Enhanced wavefront-curvature reshaping**: Multilayer progressive curvature control maintains better matching to ideal spherical wavefronts across extended distance ranges compared to single-plane constraints.
2. **Collaborative optical path regulation**: Each propagation segment and transverse position difference contributes additional path differences, maintaining sufficient inter-element phase variation throughout the Rayleigh region.
3. **Extended range-domain degree preservation**: Accurate wavefront matching preserves high effective channel rank over larger distances, maintaining range-resolution characteristics and multiplexing capability.

SIM does not alter the physical Rayleigh boundary but enhances engineering utilization of near-field resources in the middle and latter Rayleigh region portions by reducing residual phase error and improving focusing consistency.

IV. Theoretical Modeling and Analysis

A. Unified Maximum Phase Difference Expression

For arbitrary propagation path $\mathcal{P}$ from feed to observation point P, the total phase follows:

$$\Phi\left(\mathcal{P};r\right)=\frac{2\pi}{\lambda}L\left(\mathcal{P};r\right)+\sum_{l=1}^{L}\varphi_{l}\left(\mathcal{P}\right) \tag{16}$$

where $L\left(\mathcal{P};r\right)$ denotes total geometric path length and $\varphi_{l}\left(\mathcal{P}\right)$ represents coded phase at layer l.

The maximum phase difference becomes:

$$\Delta\varphi_{\max}^{(L)}(r)=\max_{\mathcal{P}_{a},\mathcal{P}_{b}\in\Omega}\left|\frac{2\pi}{\lambda}\left[L\left(\mathcal{P}_{a};r\right)-L\left(\mathcal{P}_{b};r\right)\right]+\sum_{l=1}^{L}\left[\varphi_{l}\left(\mathcal{P}_{a}\right)-\varphi_{l}\left(\mathcal{P}_{b}\right)\right]\right| \tag{17}$$

where Ω denotes the set of all reachable paths.

For focusing quality evaluation, the critical metric is residual phase error relative to ideal focused wavefront:

$$\Delta\phi_{\mathrm{res,max}}^{(L)}\left(r\right)=\max_{p_{a},p_{b}\in\Omega}\left|\left[\Phi(p_{a};r)-\Phi(p_{b};r)\right]-\left[\phi_{\mathrm{ideal}}\left(p_{a},r\right)-\phi_{\mathrm{ideal}}\left(p_{b},r\right)\right]\right| \tag{18}$$

where $\Phi(p;r)$ denotes actual synthesized wavefront phase, and $\phi_{ideal}\left(\rho,r\right)$ represents ideal focusing phase.

Under paraxial approximation with dominant aperture edge effects, residual phase error relates to curvature mismatch:

$$\Delta\phi_{\text{res,max}}^{(L)}(r) \approx \frac{\pi D^2}{4\lambda}\left|\frac{1}{R_{\text{actual}}^{(L)}} - \frac{1}{r}\right| \tag{19}$$

where $R_{eq}^{(L)}(r)$ represents equivalent radius of curvature of synthesized wavefront.

B. Near-Field Extension Factor Quantification

The normalized near-field enhancement factor is defined as:

$$\kappa_L = \frac{R_{ERF}^{(L)}}{R_{ERF}^{SL}}, \tag{20}$$

while the Rayleigh-distance coverage ratio measures boundary utilization:

$$\eta_{Ray}^{(L)} = \frac{R_{ERF}^{(L)}}{R_{Ray}}. \tag{21}$$

Under residual phase-error threshold η_{Ray}^{L} the effective boundary satisfies:

$$\eta_{Ray}^{L} = \frac{R_{ERF}^{L}}{R_{Ray}}, \quad 0 < \eta_{Ray}^{L} \leq 1 \tag{23}$$

yielding admissible curvature mismatch:

$$\frac{\pi D^2}{4\lambda}\left|\frac{1}{R_{actual}^{(L)}(R_{ERF}^{(L)})} - \frac{1}{R_{ERF}^{(L)}}\right| = \Delta\phi_{th} \tag{23}$$

The focusing-gain loss constraint requires:

$$\varepsilon^{(L)}\left(R_{ERF}^{(L)}\right) \leq \varepsilon_{th}. \tag{24}$$

SIM's capability to push $R_{ERF}^{(L)}$ toward R_{Ray} depends on maintaining small curvature mismatch and focusing-gain loss even near the Rayleigh boundary.

C. Parameter Influence and Nonideal Effects

Extension performance depends critically on layer number L, interlayer spacing s, transmission efficiency β, and phase precision. Key design insights include:

1. **Optimal layer number exists**: Increasing layers improves wavefront control degrees of freedom but introduces cascaded loss and error accumulation, typically yielding non-monotonic performance versus L.

2. **Interlayer spacing tradeoff**: Insufficient spacing limits field redistribution effects, while excessive spacing increases assembly sensitivity and propagation loss.
3. **Unit-cell performance prerequisite**: Low insertion loss and high phase precision form the foundation for realizing cascaded regulation advantages.

Nonideal factors including insertion loss, phase quantization error, assembly deviations, amplitude-phase coupling, and mutual coupling create a balance between **regulation gain** and **cascading penalty**. Performance enhancement occurs only when wavefront expression capability improvements outweigh these penalties.

D. Theoretical Discussion

Multilayer SIM architecture fundamentally differs from single-layer structures through coupled field transformation. Interlayer propagation remaps locally modulated fields into complex incident patterns for subsequent layers, creating cross-layer coupling through spherical-wave propagation. This enables richer target-field representations and stronger intermediate-field reshaping capability.

The near-field extension capability arises from:

1. **Progressive wavefront curvature control** across multiple planes, maintaining pronounced curvature over extended distances.
2. **Cross-layer optical path accumulation**, where each propagation segment contributes additional path differences for enhanced phase variation.
3. **Range-domain degree preservation**, where larger inter-element phase differences maintain channel rank and near-field advantages at longer distances.

This extension translates physical near-field existence into practical communication and sensing performance gains through improved SNR and multiplexing capability.

V. Numerical Validation

We implement scalar-field simulations using free-space Green's functions for propagation modeling. Parameters include: operating frequency 28 GHz ($\lambda \approx 10.7$ mm), aperture size $D = 10\lambda$, and 3-bit phase quantization. Systems maintain identical feed illumination and total power constraints.

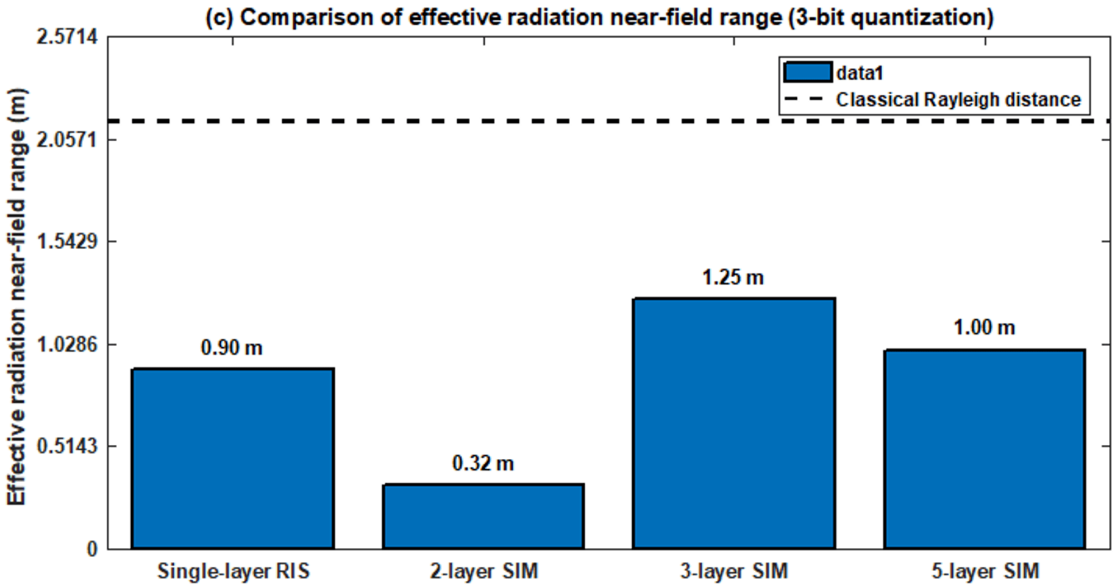

Figure 2. Comparison of the effective radiative near-field range between a single-layer RIS and SIM.

Fig. 2 compares effective radiative near-field ranges. The classical Rayleigh distance is $R_{Ray} = 2.1429$ m. Single-layer RIS achieves $R_{ERF}^{SL} = 0.9$ m (41.99% of R_{Ray}). For SIM configurations: 2-layer achieves 0.32 m (14.93%), 3-layer achieves 1.25 m (58.33%), and 5-layer achieves 1.0 m (46.67%).

Results demonstrate non-monotonic performance versus layer number due to tradeoffs between regulation gain and cascading penalties. The 3-layer configuration achieves optimal performance, significantly improving focusing quality throughout the Rayleigh region and pushing the engineering boundary closer to the physical limit. This validates SIM's capability to enhance near-field resource utilization while respecting fundamental diffraction constraints.

VI. Conclusion

This paper has systematically investigated stacked intelligent metasurfaces for extending effective radiative near-field range in 6G systems under fixed aperture constraints. Our analysis clarifies the distinction between physical boundaries and engineering performance limits, establishing three key findings:

1. The classical Rayleigh distance represents an intrinsic physical boundary determined solely by aperture size and wavelength, fundamentally constrained by diffraction limits. SIM architectures cannot alter this boundary but enhance programmable wavefront shaping to extend engineering-effective operating distance.

2. SIM performance depends critically on the balance between regulation gain and cascading penalties. Optimal designs exhibit finite layer numbers determined by interlayer spacing, insertion loss, and phase precision tradeoffs, rather than unbounded stacking.
3. Multilayer SIMs significantly improve focusing quality throughout the Rayleigh region, pushing engineering boundaries closer to physical limits and enabling practical utilization of near-field advantages for 6G communications and sensing.

This work provides theoretical foundation and numerical validation for multilayer metasurface design in 6G near-field systems. Future research will incorporate wideband effects, mutual coupling, polarization characteristics, robust optimization strategies, and experimental prototype validation to advance practical implementation.

About the Author

Zhao Yajun (Member, IEEE) holds Bachelor's, Master's, and Doctoral degrees. Since 2010, he has assumed the role of Chief Engineer within the Wireless and Computing Product R&D Institute at ZTE Corp. Prior to this, he contributed to wireless technology research within the Wireless Research Department at Huawei. Currently, his primary focus centers on 5G standardization technology and the advancement of future mobile communication technology, particularly 6G. His research pursuits encompass a broad spectrum, including reconfigurable intelligent surface (RIS), spectrum sharing, flexible duplex, CoMP, and interference mitigation. He played a key role in the establishment of the RIS TECH Alliance (RISTA) and currently serves as its Deputy Secretary-General. He is a core member in promoting the creation of the RIS Task Group under the China IMT-2030 (6G) Promotion Group and serves as its Deputy Leader. Additionally, he is a core member in leading the establishment of the Technical Committee on Reconfigurable Intelligent surfaces under the China Institute of Communications and serves as the Head of the Secretariat Group. He holds over a thousand patents in 4G LTE and 5G technologies, with dozens of them adopted as Standard Essential Patents (SEPs) in the 4G/5G standards.

References

1. ^*Zhao Y, Dai L, Zhang J, et al. (2025). "6G Near-Field Technologies White Paper 2.0." FuTURE Forum.*
2. ^*Zhao Y, Dai L, Zhang J, et al. (2024). "Near-Field Communications: Characteristics, Technologies, and Engineering." Front. Inf. Technol. Electron. Eng. **25**(12):1580–1626.*

3. ^Cui M, Dai L (2022). "Channel Estimation for Extremely Large-Scale MIMO: Far-Field Or Near-Field?" IEEE Trans. Commun. **70**(4):2663–2677.
4. ^Zhao Y (2023). "Reconfigurable Intelligent Surfaces for 6G: Applications, Challenges, and Solutions." Front. Inf. Technol. Electron. Eng. **24**(12):1669–1688.
5. ^An J, Debbah M, Cui TJ, Chen ZN, Yuen C (2025). "Emerging Technologies in Intelligent Metasurfaces: Shaping the Future of Wireless Communications." IEEE Trans. Antennas Propag. early access.
6. ^Li Q, El-Hajjar M, Xu C, An J, Yuen C, Hanzo L (2025). "Stacked Intelligent Metasurface-Based Transceiver Design for Near-Field Wideband Systems." IEEE Trans. Commun. **73**(9):8125–8139.
7. ^An J (2023). "Stacked Intelligent Metasurfaces for Efficient Holographic MIMO Communications in 6G." IEEE J. Sel. Areas Commun. **41**(8):2380–2396.
8. ^An J, Yuen C, Dai L, Di Renzo M, Debbah M, Hanzo L (2024). "Near-Field Communications: Research Advances, Potential, and Challenges." IEEE Wireless Commun. **31**(3):100–107.
9. ^An J (2024). "Stacked Intelligent Metasurface-Aided MIMO Transceiver Design." IEEE Wireless Commun. **31**(4):123–131.
10. ^Chen Q, et al. (2026). "Stacked Intelligent Metasurface Enhanced Integrated Communication and Computation." IEEE Internet Things J. **13**(7):14442–14453.
11. ^Yaghjian A (1986). "An Overview of Near-Field Antenna Measurements." IEEE Trans. Antennas Propag. **34**(1):30–45.

Declarations

Funding: No specific funding was received for this work.

Potential competing interests: No potential competing interests to declare.